Synthesis of optimal piezoelectric shunt impedances for structural vibration control.

Andrew J. Fleming[a] and S. O. Reza Moheimani[a]

[a]The School of Electrical Engineering and Computer Science, The University of Newcastle, Callaghan 2308, NSW, Australia

ABSTRACT

Piezoelectric transducers are commonly used as strain actuators in the control of mechanical vibration. One control strategy, termed piezoelectric shunt damping, involves the connection of an electrical impedance to the terminals of a structurally bonded transducer. Many passive, non-linear, and semi-active impedance designs have been proposed that reduce structural vibration. This paper introduces a new technique for the design and implementation of piezoelectric shunt impedances. By considering the transducer voltage and charge as inputs and outputs, the design problem is reduced to a standard linear regulator problem enabling the application of standard synthesis techniques such as LQG, $\mathcal{H}_2$, and $\mathcal{H}_\infty$. The resulting impedance is extensible to multi-transducer systems, is unrestricted in structure, and is capable of minimizing an arbitrary performance objective. An experimental comparison to a resonant shunt circuit is carried out on a cantilevered beam. Previous problems such as *ad-hoc* tuning, limited performance, and sensitivity to variation in structural resonance frequencies are significantly alleviated.

Keywords: Active, Piezoelectric, Shunt, Vibration, Control

1. INTRODUCTION

Active feedback control involves the use of sensors and actuators to minimize structural vibration. The vibration is sensed directly and used to derive an actuator voltage V_a counter-active to the applied disturbance. Typical vibration sensors include accelerometers, velocimeters, and strain sensors. The foremost difficulties associated with active feedback control are due mainly to the intrinsic nature of the plant G. Mechanical systems are of high order and contain a large number of lightly damped modes. The modeling and control design for such systems is well known to pose significant challenges. In addition, environmental variation of the structural resonance frequencies can further complicate the problem by compromising stability margins and restricting performance. Examples of active feedback control incorporating piezoelectric actuators can be found in references[1–3] .

In active vibration control, and many other applications, piezoelectric transducers are used exclusively as either sensors or actuators. Dosch, Inman, Garcia[4] and Anderson, Hagood, Goodliffe[5] were able to demonstrate a technique now referred to as piezoelectric self-sensing, or sensori-actuation. By subtracting the capacitive voltage drop from the applied terminal voltage, a reconstruction of the internal piezoelectric strain voltage can be obtained. The reconstructed strain voltage can be employed as an active feedback sensor effectively eliminating the need for an auxiliary transducer. In addition to the usual problems associated with active feedback control, piezoelectric self-sensing systems are also highly sensitive to the transducer capacitance value. A sensing capacitance not perfectly matched to the transducer capacitance can result in significant errors in the strain estimation. If the estimate is used within a feedback control loop, such uncertainty may severely affect performance or cause instability. An attempt to address the problem of capacitance sensitivity can be found in[6, 7] .

Another technique, first appearing in[8] , termed shunt damping, involves the connection of an electrical impedance to the terminals of a piezoelectric transducer. Impedance designs have included resistors[9] , inductive networks[10, 11] , switched capacitors[12] , switched networks[13] , negative capacitors[14] , and active impedances[15] . Shunt damping has a number of benefits and disadvantages when compared to active feedback control. Shunt circuits do not require a feedback sensor, and in some circumstances, may not require any support electronics or power supply at all. Typically, a shunt damping strategy involves a specific impedance structure which is designed to damp a number of targeted structural modes. Another advantage of shunt damping is that the circuits can be fine-tuned online to compensate for any modeling errors experienced during the design process. Automatic online tuning techniques have also been presented[16] .

E-mail: andrew@ee.newcastle.edu.au

Smart Structures and Materials 2004: Damping and Isolation, edited by Kon-Well Wang,
Proc. of SPIE Vol. 5386 (SPIE, Bellingham, WA, 2004) · 0277-786X/04/$15 · doi: 10.1117/12.539687

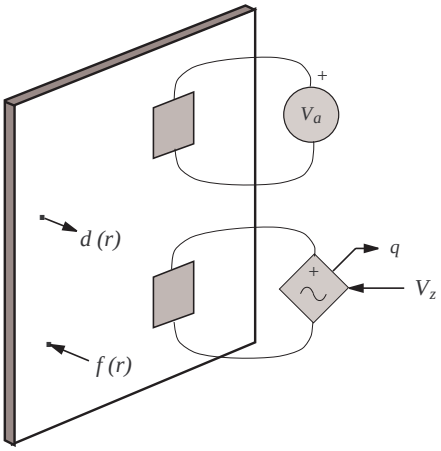

Figure 1. A general piezoelectric laminate structure excited by a distributed force $f(r,t)$ and the voltage $V_a(t)$ applied to a disturbance patch. The resulting vibration $d(r,t)$ is suppressed through the presence of an electrical impedance connected to the shunt transducer.

This paper presents a fully automatic technique for the design and implementation of piezoelectric shunt damping circuits. By viewing the transducer voltage and charge as inputs and outputs, the task of impedance design can be cast as a standard regulator problem. Synthesis techniques such as LQG, $\mathcal{H}_2$, and $\mathcal{H}_\infty$ are readily applied to procure a suitable impedance. Unlike present methodologies, the impedance is unrestricted in structure, is multi-port for multi-transducer systems, and can be designed to meet any performance specification set within the flexibility of the synthesis process.

The following two sections, Impedance Synthesis, and Modeling, review the basic concepts of impedance synthesis and introduce a simple, charge based modeling technique for piezoelectric laminate structures. Section 4 outlines the control objectives and presents $\mathcal{H}_2$, and $\mathcal{H}_\infty$ approaches to the task of impedance synthesis. Experimental results in Section 5 show superior performance to passive shunt damping circuits. The results and contributions are summarized in Section 6.

2. MODELING

With the aim of facilitating active shunt design, this section introduces a charge-based modeling technique for piezoelectric laminate structures.

Consider the piezoelectric laminate structure shown in Figure 1. Through the use of a shunt patch driven by the voltage V_z, the goal is to suppress vibration resulting from two disturbances: V_a, the voltage applied to a disturbance patch, and $f(r,t)$ a generally distributed external force. The implemented transfer function between the measured charge q and applied voltage V_z effectively presents an electrical impedance $Z(s)$ to the transducer. The remainder of this section is dedicated to modeling the interaction between structure, transducer, and impedance.

2.1. Composite piezoelectric-mechanical system

Consider the piezoelectric laminate structure shown in Figure 2 (a). The structure is disturbed by m transducers on the left side, and controlled by a further m collocated transducers on the other. Each piezoelectric transducer is modeled electrically as a capacitor C_{pm} in series with a strain-dependent voltage source v_{pm} [4, 9, 17] .

The task of modeling the composite piezoelectric-mechanical system will proceed much as that presented in[18] . The possibility of multiple transducers will be considered. To begin, let us define,

$$V_z = \begin{bmatrix} V_{z1} \\ V_{z2} \\ \vdots \\ V_{zm} \end{bmatrix} \quad V_p = \begin{bmatrix} V_{p1} \\ V_{p2} \\ \vdots \\ V_{pm} \end{bmatrix} \quad V_a = \begin{bmatrix} V_{a1} \\ V_{a2} \\ \vdots \\ V_{am} \end{bmatrix} \quad i = \begin{bmatrix} i_{z1} \\ i_{z2} \\ \vdots \\ i_{zm} \end{bmatrix} \tag{1}$$

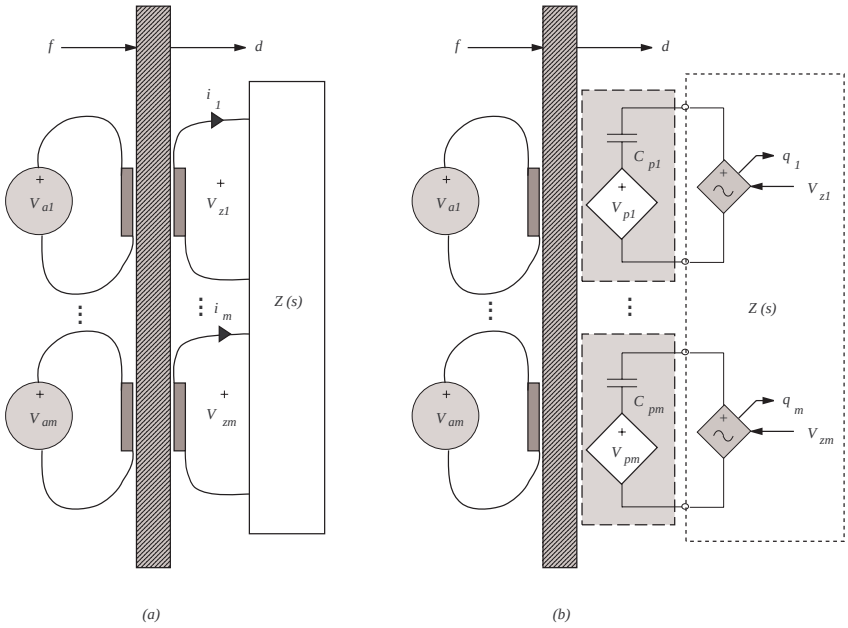

Figure 2. A shunted multi-transducer structure (a). Synthetic implementation of the impedance (b).

By applying Ohm's law, and writing Kirchoff's Voltage Law around the k^{th} loop, we obtain

$$V_z(s) = Z(s)\ i(s) \tag{2}$$

$$V_{zk}(s) = V_{pk}(s) - \frac{1}{C_{pk}s} i(s). \tag{3}$$

Assembling the results for each loop,

$$V_z(s) = V_p(s) - \frac{1}{s}\Lambda\ i(s), \tag{4}$$

$$q = -\Lambda^{-1} V_z + \Lambda^{-1} V_p, \tag{5}$$

where,

$$\Lambda = \begin{bmatrix} \frac{1}{C_{p1}} & & & \\ & \frac{1}{C_{p2}} & & \\ & & \ddots & \\ & & & \frac{1}{C_{pm}} \end{bmatrix} \tag{6}$$

After applying the principle of superposition, the strain contribution from each disturbance and shunt voltage is

$$V_p(s) = G_{av}(s) V_a(s) + G_{vv}(s) V_z(s)\ , \tag{7}$$

where $G_{va}(s)$ and $G_{vv}(s)$ are the multi-variable transfer functions from an applied disturbance and shunt voltage to the piezoelectric voltage V_p, i.e.

$$G_{va}(s) = \frac{V_p(s)}{V_a(s)} \qquad G_{vv}(s) = \frac{V_p(s)}{V_z(s)}\ . \tag{8}$$

In the case where each disturbance and shunt transducer pair are identical, collocated, and poled in opposite directions, $G_{va}(s) = -G_{vv}(s)$.

Note that this analysis does not require an equal number of disturbance and shunt transducers. This special case is considered only to allow a simplified representation of the feed-back diagram associated with the system.

The shunted composite system, alternatively referred to as the closed-loop system, can be obtained from equations (2), (3), and (7),

$$V_p(s) = \left[I - G_{vv}(s)\ Z(s)\ \left(Z(s) + \frac{1}{s}\Lambda \right)^{-1} \right]^{-1} G_{va}(s)\ V_a(s). \tag{9}$$

In a similar fashion, the composite displacement transfer function can also be derived,

$$d(r,s) = \left[I - G_{vv}(s)\ Z(s)\ \left(Z(s) + \frac{1}{s}\Lambda \right)^{-1} \right]^{-1} G_{da}(s)\ V_a(s). \tag{10}$$

where $G_{da}(s)$ is the transfer function from an applied disturbance V_a to the resulting displacement d at a point r.

The effect of a generally distributed disturbance force $f(r,s)$, and a feedback interpretation of the shunt circuit can be found in[19] .

Specific models for the transfer functions G_{va}, G_{da}, and G_{vv} will be required throughout the upcoming process of control design. The technique of modal analysis[20,21] has been used extensively throughout the literature for obtaining structural models. Under certain assumptions[20] , the force, transducer voltage, or moment applied to a linear structure can be related to the resulting sensor voltage, strain, or displacement through a transfer function of the following form,

$$G(s) = \sum_{k=1}^{\infty} \frac{\Psi_k}{s^2 + 2\varsigma_k\omega_k s + \omega_k^2}, \tag{11}$$

where $G(s)$ is intuitively parameterized by the structural resonance frequencies ω_k, modal damping ratios ς_k, and vector coefficients Ψ_k. In practical applications, where only the first N modes are of importance, the summation is usually truncated accordingly. A feed-through term D is included to correct in-bandwidth zero locations that are perturbed by the truncation of higher order modes[22] . Hence, we define the system transfer function G_{vv} as

$$G_{vv}(s) = \sum_{k=1}^{N} \frac{\Psi_k^{vv}}{s^2 + 2\varsigma_k\omega_k s + \omega_k^2} + D_{vv}. \tag{12}$$

Likewise for the transfer functions G_{va}, G_{da}, G_{df} and G_{vf}.

2.2. Abstracted plant model

The general input-output model of a piezoelectric laminate structure is shown in Figure 3. In conformance with the standard MIMO control formulation, the plant contains two sets of inputs: the disturbance signals w, and the control signals u. For the case under consideration, the disturbance and control signals are realized through a set of voltages V_a and V_z applied to a number of laminated piezoelectric patches. The system outputs V_p, $d(r,t)$, and q, correspond respectively to the piezoelectric voltages induced in each shunt patch, the dynamic displacement measured at a point r, and the charge resident on each patch. The displacement signal $d(r,t)$ is chosen as our performance variable z, while the measured charge q is our feedback variable y. Although the induced shunt piezoelectric voltages V_p are not required during the design, their inclusion aids in the modeling process. Given a specific s-impedance, the signal V_p also allows us to compute the equivalent collocated active feedback controller. A state-space realization of (12) is easily generated to represent the system P.

$$\begin{aligned} \dot{x} &= \mathbf{A}x + \mathbf{B} \begin{bmatrix} V_a \\ V_z \end{bmatrix} \\ \begin{bmatrix} V_p \\ d(r) \\ q \end{bmatrix} &= \mathbf{C}x + \mathbf{D} \begin{bmatrix} V_a \\ V_z \end{bmatrix} \end{aligned} \tag{13}$$

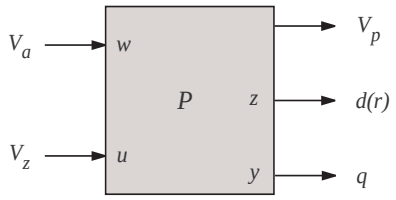

Figure 3. The composite structural piezoelectric plant P.

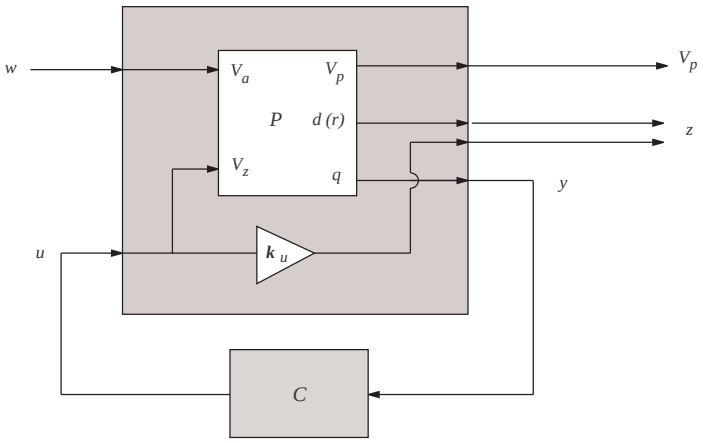

Figure 4. The standard $\mathcal{H}_2$ and $\mathcal{H}_\infty$ design problem containing the composite plant P and a secondary performance signal weighting the applied shunt voltage V_z.

where,

$$\mathbf{A} = \begin{bmatrix} 0 & 1 & & & \\ -\omega_1^2 & -2\varsigma_i\omega_1^2 & & & \\ & & \ddots & & \\ & & & 0 & 1 \\ & & & -\omega_N^2 & -2\varsigma_N\omega_N^2 \end{bmatrix} \qquad \mathbf{B} = \begin{bmatrix} \mathbf{B}_1 & \mathbf{B}_2 \end{bmatrix} = \begin{bmatrix} 0 & 0 \\ F_1 & H_1 \\ \vdots & \vdots \\ 0 & 0 \\ F_N & H_N \end{bmatrix} \tag{14}$$

$$\mathbf{C} = \begin{bmatrix} \mathbf{C}_1 \\ \mathbf{C}_2 \\ C_p\mathbf{C}_1 \end{bmatrix} = \begin{bmatrix} E_1 & 0 & \cdots & E_N & 0 \\ 1 & 0 & \cdots & 1 & 0 \\ C_pE_1 & 0 & \cdots & C_pE_N & 0 \end{bmatrix} \qquad \mathbf{D} = \begin{bmatrix} D_{11} & D_{12} \\ D_{21} & D_{22} \\ D_{11}C_p & -C_p + D_{12}C_p \end{bmatrix} \tag{15}$$

where F_k and H_k $k \in \{1, 2, \cdots N\}$ are the state-input weightings of each disturbance and shunt transducer. The vectors E_k $k \in \{1, 2, \cdots N\}$ represent the contribution of each mode to the induced piezoelectric voltages.

As an alternative to the parameterized modeling approach presented above, a multi-variable time or frequency domain system identification technique could be employed to estimate the plant P directly from experimental data.

3. S-IMPEDANCE CONTROL DESIGN

Given the composite model discussed in Section 2, the problem of designing an appropriate impedance can be cast as a standard $\mathcal{H}_2$ or $\mathcal{H}_\infty$ regulator problem. As shown in Figure 4, the regulator $C(s)$ accepts the measured charge q to provide a control signal V_z counteractive to the applied disturbance V_a. The objective is to minimize the structural displacement $d(r, t)$ subject to a weighting on the magnitude of the required terminal voltage V_z.

In an $\mathcal{H}_2$ sense, the goal is to minimize the transfer function from an applied disturbance w to the performance signal z, i.e. we seek to minimize

$$J = \left\| \frac{z(s)}{w(s)} \right\|_2 = \left\| \frac{d(r,s) + \mathbf{k}_u V_z(s)}{V_a(s)} \right\|_2 . \tag{16}$$

where the $\mathcal{H}_2$ norm $\|F(s)\|_2$ of $F(s)$ is defined as

$$\|F(s)\|_2^2 = \frac{1}{2\pi} \int_{-\infty}^{\infty} tr\left\{F(j\omega)F(j\omega)'\right\}\ d\omega. \tag{17}$$

By Parseval's equality, the optimal $\mathcal{H}_2$ controller minimizes the expected root-mean-square (RMS) value of z. An optimal $\mathcal{H}_2$ controller can be found through the solution of an algebraic Ricatti equation.

Disadvantages associated with $\mathcal{H}_2$ and LQG methods include the unrealistic Gaussian disturbance model, and problems related to integral performance constraints. $\mathcal{H}_\infty$ optimization and robust control, originally championed by Zames[23] , is an alternative to $\mathcal{H}_2$ and LQG methods.

Applying $\mathcal{H}_\infty$ control to the problem of s-impedance synthesis involves finding a controller $C(s)$ that minimizes

$$J = \left\| \frac{z(s)}{w(s)} \right\|_\infty = \left\| \frac{d(r,s) + \mathbf{k}_u V_z(s)}{V_a(s)} \right\|_\infty . \tag{18}$$

where the $\mathcal{H}_\infty$ norm $\|F(s)\|_\infty$ of $F(s)$ is defined as

$$\|F(s)\|_\infty = \max_\omega\ \bar{\sigma}\left(F(j\omega)\right) \tag{19}$$

where $\bar{\sigma}$ denotes the maximum singular value.

In the time domain, $\mathcal{H}_\infty$ control can be interpreted as minimizing the worst-case induced 2-norm of z, i.e.

$$\left\| \frac{z(s)}{w(s)} \right\|_\infty = \max_{w(t)\neq 0}\ \frac{\|z(t)\|_2}{\|w(t)\|_2} \tag{20}$$

where $\|f(t)\|_2^2 = \int_0^\infty \sum_i |f_i(t)|^2\ dt$.

Closely resembling the solution to $\mathcal{H}_2$ synthesis, an optimal $\mathcal{H}_\infty$ controller can be found through the solution of an algebraic Ricatti equation[24, 25] .

Linear Quadratic Gaussian methods (LQG) are also readily applied[19] .

4. EXPERIMENTAL RESULTS

In the following sub-sections, an $\mathcal{H}_\infty$ s-impedance controller is designed and applied experimentally to control a piezoelectric laminate cantilever beam.

4.1. Experimental Apparatus

The experimental apparatus, shown in Figure 6 and pictured in Figure 5, consists of a uniform aluminium cantilever beam. Three piezoelectric transducers are laminated onto the front face and connected electrically in series to the voltage source V_z. A single collocated disturbance transducer, identical to each of the shunt transducers, is also mounted on the back face and driven with the disturbance voltage V_a. Physical parameters of the beam and piezoelectric transducers can be found in Tables 1 and 2.

The displacement measurement $d(r,t)$ is acquired using a Polytec PSV300 scanning laser vibrometer.

4.1.1. Voltage Driver with Charge Instrumentation

Details of a voltage amplifier with charge instrumentation can be found in[19] .

4.2. Parameter Identification

To determine the model parameters shown in equation (13), a simple optimization scheme is employed. From an initial guess, ω_i and ς_i, are found through a simplex optimization based on the measured disturbance to displacement transfer function $\frac{d(r,s)}{V_a(s)}$, i.e.

$$\begin{bmatrix} \omega_k & \varsigma_k \end{bmatrix} = \arg \min \left\| \tilde{P}_{dV_a}(s) - P_{dV_a}(s) \right\|_2, \tag{21}$$

where $\tilde{P}_{dV_a}(s)$ is the measured transfer function from an applied disturbance $V_a(s)$ to the displacement $d(r,s)$. With these parameters in hand, those remaining are determined from a final global optimization,

$$\arg \min \left\| \tilde{P}(s) - P(s) \right\|_{2,\,W} . \tag{22}$$

As gains from channel to channel vary greatly, a multivariable frequency weight W is required to normalize the cost of each error transfer function.

The magnitude and phase response of the measured system and resulting model are shown in Figures 7 and 8. The model is an accurate representation of the measured system. Note the close pole-zero spacing in the transfer function from an applied shunt voltage V_z to the charqe q. Referring to Eq (15), this behaviour is due to the transducer capacitance which results in a large direct feed-through.

In the following sections it will be of interest to examine the robustness of each control strategy to a change in the structural resonance frequencies. Experimentally, such variation is accomplished by affixing a mass 60 mm from the beam tip. The corresponding change in structural resonance frequencies is illustrated in Figure 9.

4.3. Passive Shunt Design

For the sake of comparison, each LQG and $\mathcal{H}_\infty$ shunt impedance will be judged against a traditional resonant piezoelectric shunt damping circuit applied to the same structure. A current-flowing shunt circuit[26] was designed and tuned to minimize the $\mathcal{H}_2$ norm of the cantilever beam. The schematic and component values can be found in Figure 10 and Table 3.

4.4. $\mathcal{H}_\infty$ Shunt Design

This sub-section documents the design and implementation of an $\mathcal{H}_\infty$ s-impedance. As discussed in Section 3, an $\mathcal{H}_\infty$ s-impedance is designed to minimize the following cost function,

$$J = \left\| \frac{d(r,s) + k_u V_z(s)}{V_a(s)} \right\|_\infty , \tag{23}$$

where k_u, the control signal weighting, was chosen to be 3.2×10^{-7}. A random auxiliary input of negligible influence was also included to avoid plant inversion. For a discussion on plant inversion and its avoidance, see Fleming 2004[19] .

The complex s-impedance of the resulting $\mathcal{H}_\infty$ controller is plotted in Figure 11.

Examining the open- and closed-loop pole locations shown in Figure 12, the controller is clearly augmenting the system damping. Corresponding mitigation of the transfer function from an applied disturbance to the measured displacement can be seen in both the frequency domain, Figure 13, and the time domain, Figure 15. The magnitude of the first and second structural modes are reduced by 30.3 and 24.0 dB respectively. Damping ratios are increased from 0.00246 and 0.0011 to 0.0288 and 0.00766.

An unexpected feature of the s-impedance is its smooth frequency response; there are no localized peaks at the resonance frequencies. In contrast, active strain-, velocity-, or acceleration-feedback controllers characteristically apply a highly localized gain at the frequencies of structural resonance. In the advent of model variation, such localized behavior can result in considerable performance degradation. In order to examine system robustness, the nominal system is perturbed by adding a mass 60 mm from the beam tip. Aside from the disturbance to the underlying partial differential equation, the first and second resonance frequencies are decreased by 13.5 and 2.2 % respectively. The consequence on both passive and active shunt circuits is shown in Figure 14. While the $\mathcal{H}_\infty$ shunt loses only 3.3 and 0.8 dB from its unperturbed attenuation of the first and second modes, the passive shunt loses 13.4 and 4.8 dB. Corresponding time domain results are shown in Figure 15.

Length, L	376 mm
Thickness, h	3 mm
Width, W	50 mm
Density, ρ	2.770×10^{3} kg/m^3
Young's Mod., E	7.00×10^{10} N/m^2

Table 1. Beam Parameters

Length, L_{pz}	50 mm
Thickness, h_{pz}	0.25 mm
Width, W_{pz}	15 mm
Charge Constant, d_{31}	-210×10^{-12} m/V
Voltage Constant, g_{31}	-11.5×10^{-3} Vm/N
Coupling Coefficient, k_{31}	0.34
Capacitance, C_p	43 nF
Young's Mod., E_{pz}	63×10^{9} N/m^2

Table 2. Properties of the Physik Instrumente Transducers (PIC151 Ceramic)

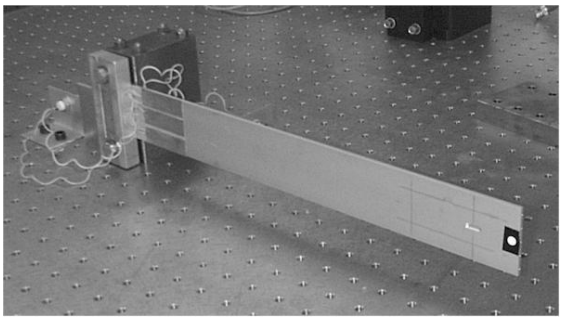

Figure 5. The cantilever beam.

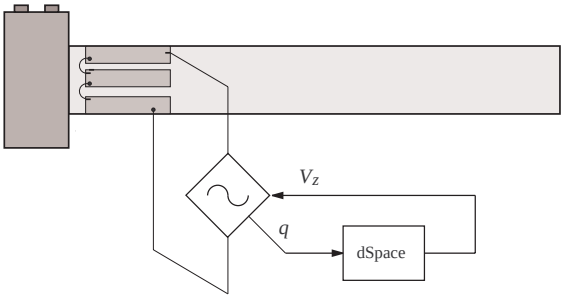

Figure 6. A front elevation of the cantilever beam. A single co-located disturbance transducer excited by the voltage V_a, is also mounted on the back face.

C_1	10 nF	C_2	10 nF
L_1	11690 H	L_2	348 H
R_1	15 $k\Omega$	R_2	9 $k\Omega$

Table 3. Component values of the current-flowing shunt circuit.

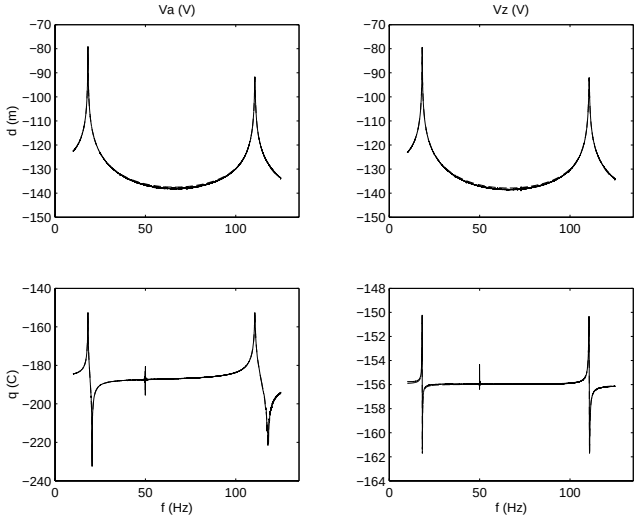

Figure 7. The simulated (- -) and experimental (—) magnitude frequency response (in decibels) of the shunt voltage controlled piezoelectric beam.

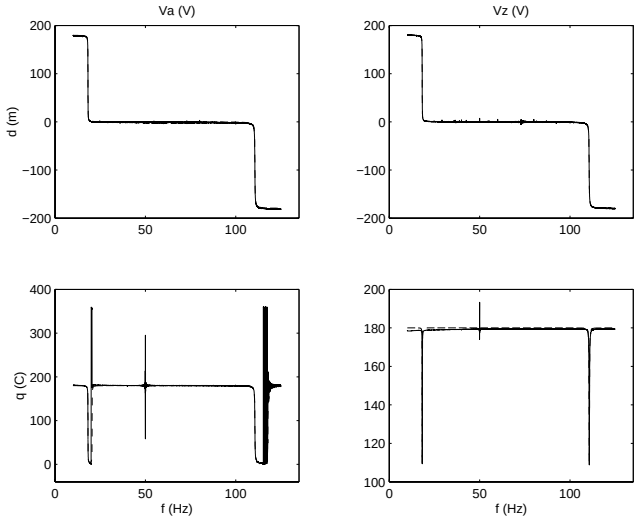

Figure 8. The simulated (- -) and experimental (—) phase frequency response (in degrees) of the shunt voltage controlled piezoelectric beam.

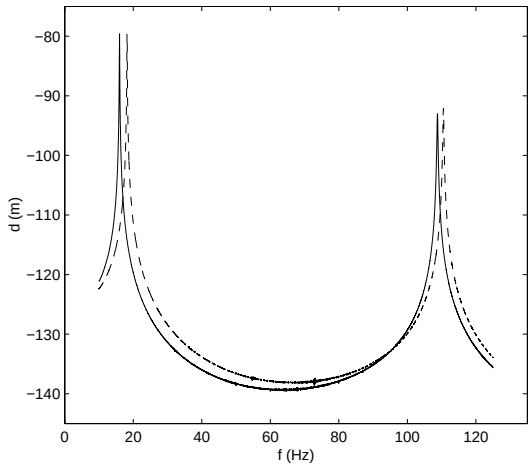

Figure 9. The experimental frequency response (in decibels) from an applied disturbance voltage V_a (V) to the resulting tip displacement d (m). Free (- -), With Mass (—).

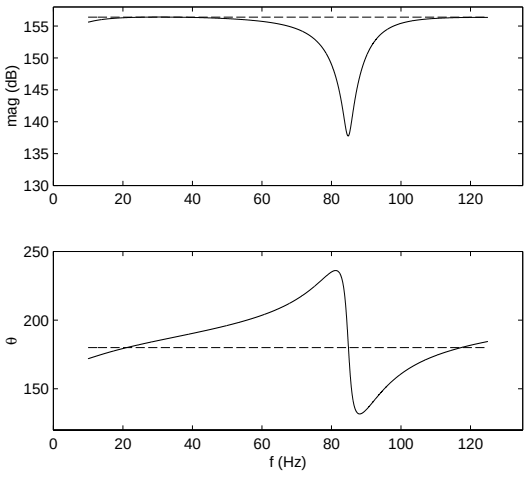

Figure 11. Complex s-impedance of the $\mathcal{H}_\infty$ (—), and ideal negative capacitor (- -) shunt controller.

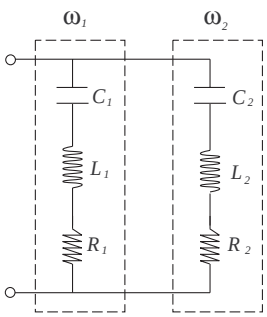

Figure 10. A dual-mode current-flowing piezoelectric shunt damping circuit.[26]

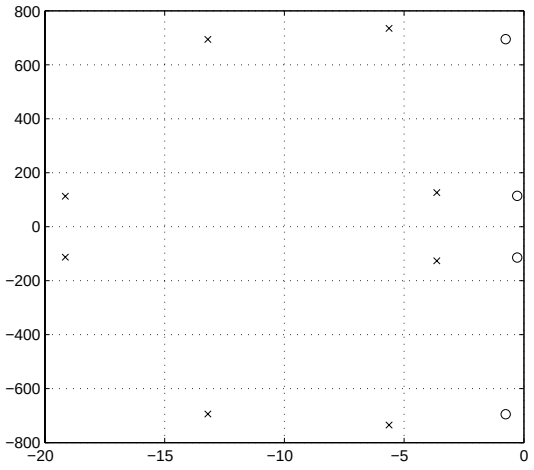

Figure 12. The open- (◯), and closed-loop (×) pole locations of the $\mathcal{H}_\infty$ shunt controlled system.

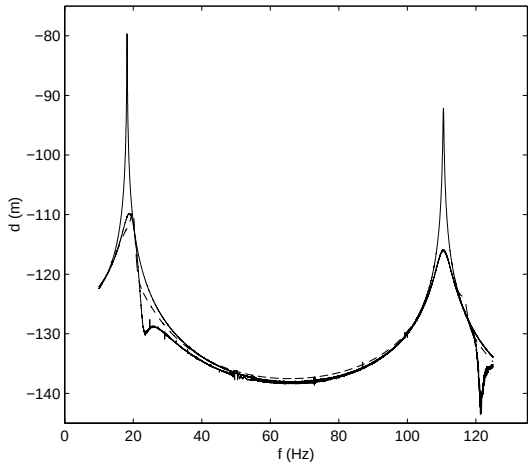

Figure 13. The experimental (—), and simulated (- -), $\mathcal{H}_\infty$ shunt controlled frequency responses (in decibels) from an applied disturbance voltage V_a (V) to the resulting tip displacement d (m). The open-loop response is also shown (—).

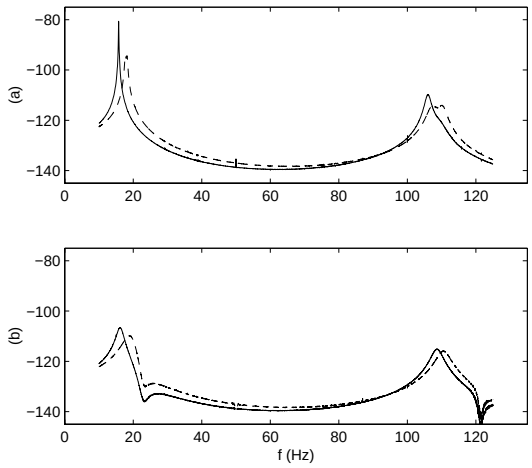

Figure 14. The free (- -), and with-mass (—), passive (a) and $\mathcal{H}_\infty$ shunt controlled (b) experimental frequency responses (in decibels) from an applied disturbance voltage V_a (V) to the resulting tip displacement d (m).

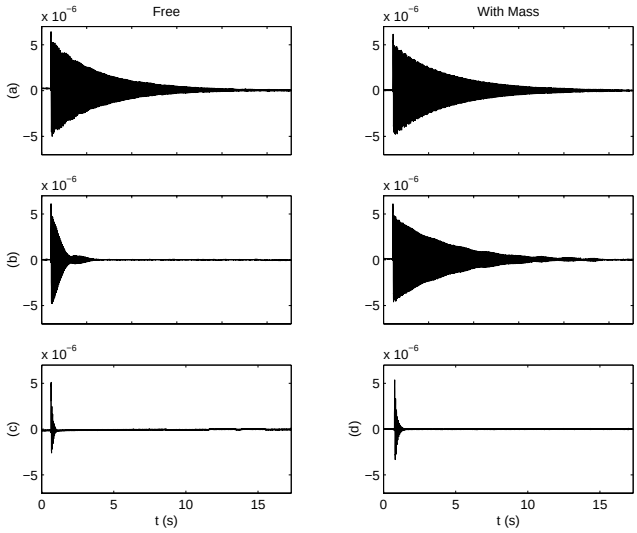

Figure 15. The free (left column) and with-mass (right column) tip displacement response d (m) to a step disturbance in V_a. Experimental open-loop (a), passive shunt controlled (b), and $\mathcal{H}_\infty$ shunt controlled (c) systems.

5. CONCLUSIONS

A framework has been presented for the design of active shunt impedances. By viewing a piezoelectric laminate structure as a system with transducer voltage inputs and charge outputs, the task of shunt impedance design can be accomplished through the solution of a standard control problem e.g. by LQG, $\mathcal{H}_2$, or $\mathcal{H}_\infty$ synthesis. The resulting controller, effectively the derivative of impedance, can be implemented directly with a voltage amplifier and charge measurement.

Although the fundamental goal in smart structure design is often to the augment system damping, this cannot be specified directly as an LQG, $\mathcal{H}_2$, or $\mathcal{H}_\infty$ performance objective. The approach has been to achieve this indirectly through mitigation of the performance transfer function $\frac{d(s)}{V_a(s)}$.

Experimentally, the active shunts have proven to introduce significant system damping, up to 30.3 dB attenuation of the first cantilever mode.

While achieving levels of performance previously only available through sensor-based feedback control, active shunt impedances are remarkably insensitive to variation in the structural resonance frequencies. A 13.5 % change in the first resonance frequency resulted in only a slight loss in performance. By comparison, the same variation had a disastrous consequence on the performance of a passive shunt damping circuit. Such sensitivity has limited the practical application of smart structures incorporating either active feedback or passive shunt vibration control systems.

Another well known problem associated with passive shunt damping is the lack of control influence. Given a lightly damped structure, even the small counteractive forces associated with passive shunt circuits can significantly increase system damping. Many practical mechanical structures naturally exhibit higher levels of damping. In such cases, passive piezoelectric shunt circuits are of limited use. As the amount of control influence associated with active shunt impedances is arbitrary, the possibility now exists for controlling more heavily damped systems. In such cases, the control voltage V_z is expected to become quite large. At high drive voltages it may be necessary to address the inherent piezoelectric hysteresis.

The reader will appreciate that the presented techniques are quite general and valid for structures incorporating multiple piezoelectric transducers. Although the application of sensor-based feedback control is well defined and feasible for structures with multiple sensors and actuators, the same can not be said for multi-transducer shunt circuits[18] . Present multi-transducer, multi-mode shunt circuits are simply a direct extension of single transducer shunt circuits. Each circuit is restricted to be independent and attached to a single transducer. If a single mode is to be targeted by two or more transducers, the task of tuning the shunt circuit can become extremely tedious. In addition to the complicated interaction between transducers at those frequencies, there are now as many more tuning parameters as there are transducers per mode. The design freedom afforded with active shunts not only eliminates the complicated task of tuning, but allows for full utilization of each patch. The resulting impedance is unstructured, multivariable, and able to exploit benefits that may arise from inter-transducer coupling.

Possible applications of active piezoelectric shunt impedances include sensor-less, high performance vibration control of acoustic panels, flexible structures, and positioning systems. Future work includes multi-transducer structures and restricted impedance design. The LQG and $\mathcal{H}_\infty$ impedance designs contained negative reactive components and are unstable in a systems perspective. Although the connection of the transducer and control impedance is stable, an inherently stable controller is desirable. It is presently unclear if an unstable controller is necessary to result in effective vibration reduction.

REFERENCES

1. E. Garcia, J. D. Dosch, and D. J. Inman, "Vibration attenuation in an active antenna structure," in *Proc. Conference on recent advances in active control of sound and vibration*, pp. S35–S42, (Viginia Polytechnique Institute and State University, Blacksburg), April 15-17 1991.
2. N. W. Hagood, W. H. Chung, and A. von Flotow, "Modelling of piezoelectric actuator dynamics for active structural control," *Journal of Intelligent Material Systems and Structures* **1**, pp. 327–354, 1990.
3. K. B. Lazarus and E. F. Crawley, "Multivariable active lifting surface control using strain actuation: analytical and experimental results," in *Proc. 3rd International conference on adaptive structures*, pp. 87–101, (San Diego, CA), 1992.
4. J. J. Dosch, D. J. Inman, and E. Garcia, "A self-sensing piezoelectric actuator for collocated control," *Journal of Intelligent Material Systems and Structures* **3**, pp. 166–185, January 1992.

5. E. H. Anderson, N. W. Hagood, and J. M. Goodliffe, "Self-sensing piezoelectric actuation: Analysis and application to controlled structures," in *Proc. AIAA/ASME/ASCE/AHS/ASC Structures, Structural Dynamics, and Materials*, pp. 2141–2155, 1992.
6. J. S. Vipperman and R. L. Clark, "Hybrid analog and digital adaptive compensation of piezoelectric sensoriactuators," in *Proc. AIAA/ASME Adaptive Structures Forum*, pp. 2854–2859, (New Orleans, LA), 1995.
7. S. Acrabelli and A. Tonoli, "System properties of flexible structures with self-sensing piezoelectric transducers," *Journal of sound and vibration* **235**(1), pp. 1–23, 2000.
8. R. L. Forward, "Electronic damping of vibrations in optical structures," *Applied Optics* **18**, pp. 690–697, March 1979.
9. N. W. Hagood and A. Von Flotow, "Damping of structural vibrations with piezoelectric materials and passive electrical networks," *Journal of Sound and Vibration* **146**(2), pp. 243–268, 1991.
10. S. Y. Wu and A. S. Bicos, "Structural vibration damping experiments using improved piezoelectric shunts," in *Proc. SPIE Smart Structures and Materials, Passive Damping and Isolation, SPIE Vol. 3045*, pp. 40–50, March 1997.
11. S. Behrens, S. O. R. Moheimani, and A. J. Fleming, "Multiple mode passive piezoelectric shunt dampener," in *Proc. IFAC Mechatronics 2002*, (Berkerley, CA), December 2002.
12. L. R. Corr and W. W. Clark, "Comparison of low-frequency piezoelectric switching shunt techniques for structural damping.," *IOP Smart Materials and Structures* **11**, pp. 370–376, 2002.
13. C. Richard, D. Guyomar, D. Audigier, and H. Bassaler, "Enhanced semi-passive damping using continuous switching of a piezoelectric devices on an inductor.," in *Proc. SPIE Smart Structures and Materials, Damping and Isolation, SPIE Vol. 3989*, pp. 288–299, (Newport Beach, CA), March 2000.
14. S. Y. Wu, "Broadband piezoelectric shunts for structural vibration control." Patent No. 6,075,309, June 2000.
15. S. Behrens, A. J. Fleming, and S. O. R. Moheimani, "A broadband controller for piezoelectric shunt damping of structural vibration," *IOP Smart Materials and Structures* **12**, pp. 18–28, January 2003.
16. D. Niederberger, M. Morari, and S. Pietrzko, "Adaptive resonant shunted piezoelectric devices for vibration suppression," in *Proc. SPIE Smart Structures and Materials 2003: Damping and Isolation, SPIE Vol. 5052*, (San Deigo, CA), March 2003.
17. C. C. Won, "Piezoelectric transformer," *Journal of Guidancce, Control, and Dynamics* **18**(1), pp. 96–101, 1995.
18. S. O. R. R. Moheimani, S. Behrens, and A. J. Fleming, "Dynamics and stability of wideband vibration absorbers with multiple piezoelectric transducers," in *IFAC Mechatronics*, (Berkeley, CA), December 9-11 2002.
19. A. J. Fleming, *Synthesis and Implementation of Sensor-less Shunt Controllers for Piezoelectric and Electromagnetic Vibration Control*. PhD thesis, The University of Newcastle, Callaghan 2308, Australia, February 2004.
20. L. Meirovitch, *Elements of Vibration Analysis*, McGraw-Hill, Sydney, 2nd ed., 1996.
21. A. R. Fraser and R. W. Daniel, *Pertubation Techniques for Flexible Manipulators*, Kluwer Academic Publishers, 1991.
22. S. O. R. Mohiemani, "Minimizing the effect of out-of-bandwidth dynamics in the models of reverberant systems that arise in modal analysis: Implications on spatial H_∞ control.," *Automatica* **36**, pp. 1023–1031, 2000.
23. G. Zames, "Feedback and optimal sensitivity: Model reference transformations, multiplicitive seminorms, and approximate inverse," *IEEE Transactions on automatic control* **AC-26**, pp. 301–320, 1981.
24. J. C. Doyle, K. Glover, P. Khargonekar, and B. Francis, "State-space solutions to standard $\mathcal{H}_2$ and $\mathcal{H}_\infty$ problems," *IEEE Transactions on Automatic Control* **34**, pp. 831–847, August 1989.
25. J. C. Doyle, B. A. Francis, and A. R. Tannenbaum, *Feedback Control Theory*, Macmillan Pub. Co., New York, 1992.
26. S. Behrens, S. O. R. Moheimani, and A. J. Fleming, "Multiple mode current flowing passive piezoelectric shunt controller," *Journal of Sound and Vibration* **266**, pp. 929–942, October 2003.